Gaseous detectors

Peter H. Hansen

University of Copenhagen

Content

Example: The ATLAS TRT

Detection of ionization

Electron drift in gases

Performance of gaseous detectors

Example: The ALEPH TPC

Thin gap chambers, MSGC, GEM

The Transition Radiation Tracker

- Gaseous track detectors provide an economically feasible way to measure charged-particle trajectories of over large areas, i.e. far from the production vertex of the charged tracks from a high energy reaction.
- They localize and measure the primary ionization produced by the charged particle in the gas.
- The ATLAS Transition Radiation Tracker serves for charged particle tracking far from the beam axis and for electron identification. For this we need:
  - High granularity electrodes
  - Low noise
  - Many high precision coordinates on each track
  - Radiation hardness
  - Fast readout
  - Good e/π separation

TRT global parameters

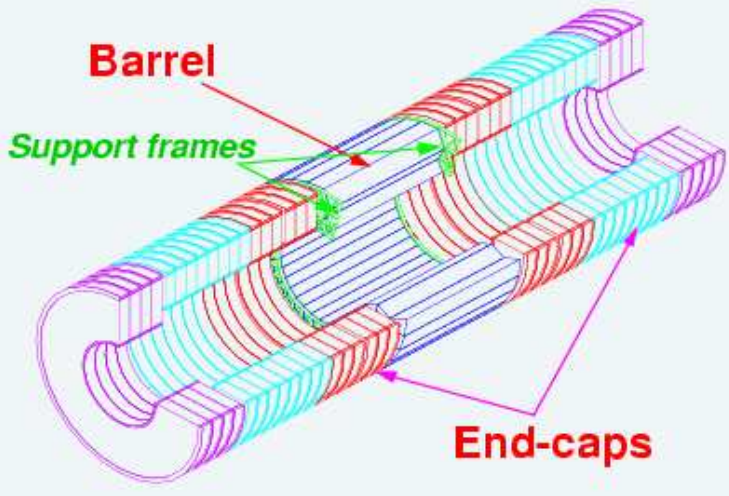

Length:	Total	6802 cm	N straws:	Total	372032
	Barrel	148 cm		Barrel	52544
	End-cap	257 cm		End-cap	319488
Outer diameter		206 cm	N electronics channels		424576
Inner diameter		96-128 cm	Weight		~1500 kg

Detail of TRT barrel

This has lead to a detector composed of some 400000 4mm straw tubes with drift-time readout. The straws are interspersed with thin polystyrene fibers and foam, causing transition radiation in the X-ray domain.

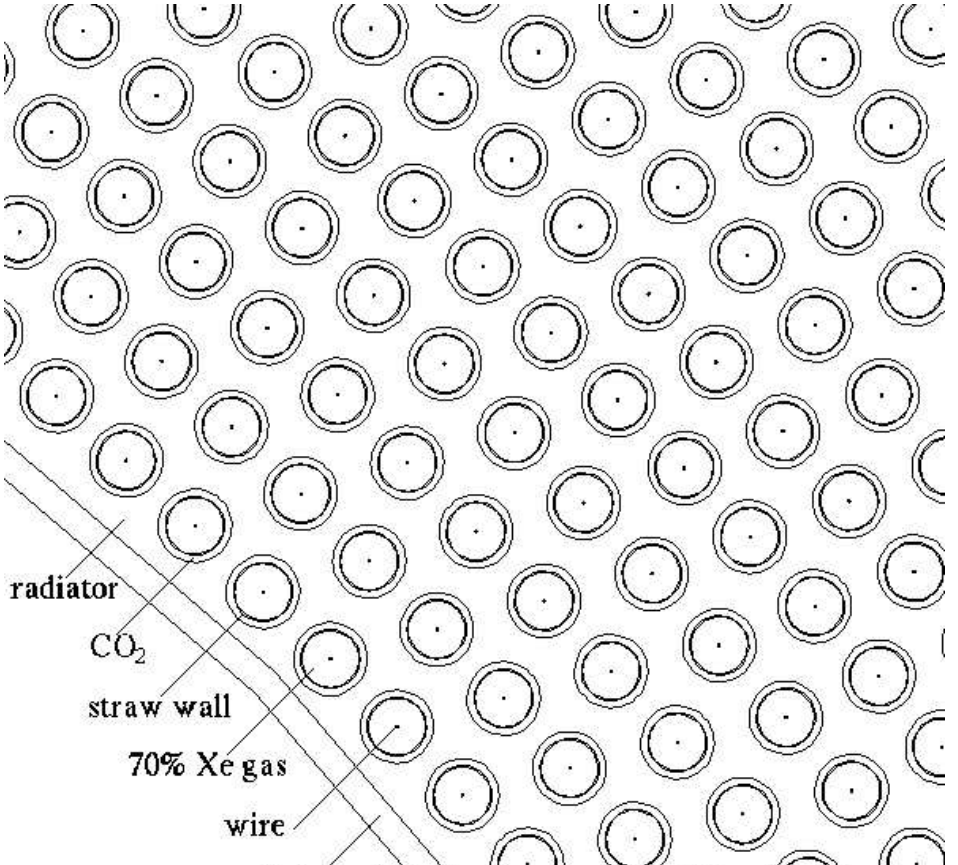

The TRT Straw

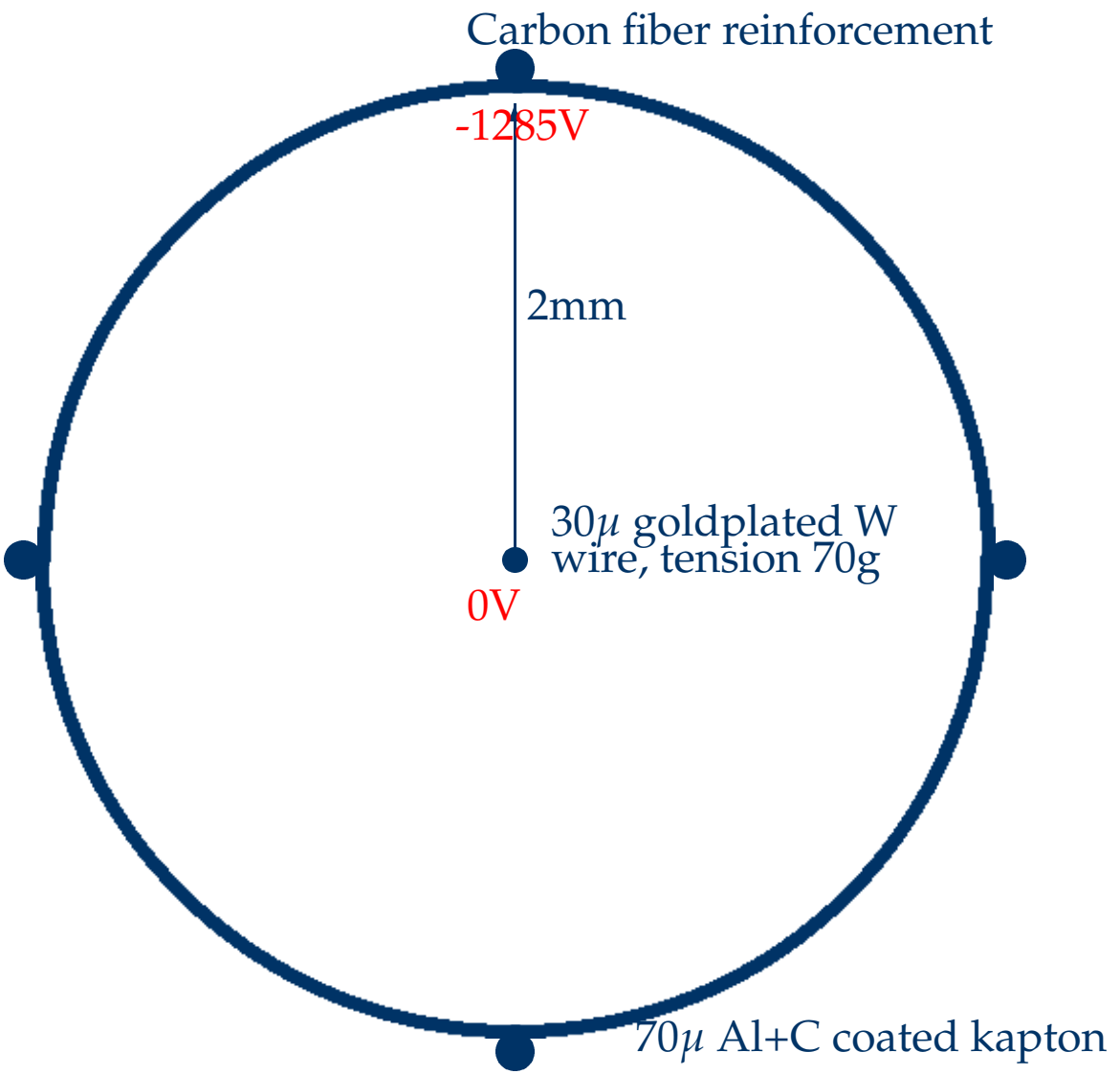

Gas proportional counters

- A proportional counter uses the avalance of secondary ionization occurring near a small-area anode to provide amplification of the primary ionization, created by a charged particle.
- In the proportional mode of high voltage on the anode, the amplified signal is still proportional to the original deposited ionization.
- At higher voltages, proportionality is lost by space-charge field distortions and the avalances starts propagate all over the counter via
  - ultra-violet photons emitted in the avalance
  - emission of electrons from positive ions being neutralized at the cathode

  This is the Geiger-Müller mode (See e.g./ Sauli Fig 49-50, Leo Fig 6.2-6.4).

Design considerations

- A gas ionization detector can have various geometries. The original cylindrical design is like the TRT straw. See Leo Fig 6.1. In other colliding beam designs, field shaping wires replace the straw. Planar geometries are discussed later.
- The geometry and the readout-scheme are sometimes arranged so that information on two perpendicular coordinates is obtained for the charged track crossing the detector. More on that later.
- The gas mixture always includes a noble gas to provide sufficient amplification and a quencher to intercept ultra-violet photons and electrons emitted at the cathode. (See Leo Sect 6.5.2 and Sauli Sect 5.3).

The TRT gas

- 70% Xe
  high amplification: $A = 2.5\ 10^4$ and X-ray absorpsion.
- 20% CO_2
  Quencher of ultra-violet photons which does not polymerize in high radiation.
- 10% O_2
  Also good at intercepting stray electrons.
- This gas has a maximum drift time of 42ns. Other properties are (at STP):

Gas	Z	A	ρ (g/cm^3)	E_{min} (eV)	W_i (eV)	$(dE/dx)_{min}$ (MeV/gcm^{-2})	n ions
Xe	54	131.3	$5.49\ 10^{-3}$	8.4	22	1.23	4
CO_2	22	44	$1.86\ 10^{-3}$	5.2	33	1.62	3

Straw detection efficiency

- For a circle with radius 2mm, the average length traversed by the charged tracks is $l = 2.7mm$. Using the Table we get an average total number of ions $n_{\text{tot}} \approx 60$ and an average number of primary ions $n_p \approx 10$.
- A primary ion is detected with almost 100% efficiency. Thus there is only serious inefficiency (of order $1/e$) when the traversed length is less than 0.27mm, i.e. 0.02mm from the straw-wall. Thus we expect a detection efficiency of 99%.

The electric field

- According to Gauss' law, the electric field is given by the capacity per unit length C and the positive voltage on the anode V_0:

$$E(r) = \frac{CV_0}{2\pi\epsilon_0 r}$$

- Integrating from the outer radius $b = 2\text{mm}$ to the radius of the wire $a = 0.015\text{mm}$, and equating the result with V_0, we get

$$\begin{aligned} E(r) &= \frac{V_0}{\log(b/a)}\frac{1}{r} = \frac{0.2V_0}{r} \\ C &= \frac{2\pi\epsilon_0}{\log(b/a)} = 0.114\ \text{pf/cm} \end{aligned}$$

Time development of the avalance

- According to a simple electrostatic argument, the moving of a charge, Q, by a distance dr in a system with capacitance per unit length C gives rise to a signal v:

$$v = \frac{Q/l}{CV_0}\frac{dV}{dr}dr$$

/

- The avalance electrons are basically all created in the last mean free path:

$$v^- = -\frac{Q/l}{CV_0}\int_a^{a+\lambda}\frac{dV}{dr}dr = -\frac{Q/l}{2\pi\epsilon_0}\log\frac{a+\lambda}{a}$$

The time development

- The positive ions drifting to the cathode gives rise to:

$$v^+ = -\frac{Q/l}{CV_0}\int_{a+\lambda}^{b}\frac{dV}{dr}dr = -\frac{Q/l}{2\pi\epsilon_0}\log\frac{b}{a+\lambda}$$

  This contribution to the signal is of order 50 times larger than that from the electrons. But it is slow, due to the slow drift of the positive ions.

- By terminating the wire in a resistance, the signal is differentiated with a time constant, $\tau_{\text{rise}} = RC$ (see Leo Fig 8.6).
  For the TRT, the rise-time is 8ns and the duration 20 about ns.

The amplification - naive calculation

- In any cascade process, we have

$$\frac{dN}{dr}(r) = \alpha(r) * N(r)$$

leading to a total amplification of:

$$A = \exp\left|\int_{r_{\text{thresh}}}^{r_{\text{anode}}} \alpha(r)dr\right|$$

- Naively, Xe atoms have about 2Å radius and drift electrons have a constant mean free path:

$$\lambda = \frac{1}{N\pi r_{Xe}^2} = 3\,10^{-5}\text{cm}, \text{ where } N = 2.5\,10^{19} \text{ atoms per cm}$$

The amplification - naive calculation

- The distance from the wire, where the avalance starts, is given by:

$$eE(r_{start})\lambda = W \Rightarrow r_{start} = \frac{0.2V_0}{22\ \mathrm{V}} 3\ 10^{-5} cm = 0.06\mu\ \frac{V_0}{22\ \mathrm{V}}$$

- The Townsend coefficient, α, is assumed to be proportional to the kinetic energy of the electrons

$$\alpha(r) = kN\epsilon(r) = kNeE(r)\lambda$$

The amplification - naive calculation

- Assuming $\alpha = \log 2/\lambda = 2.3\ 10^4$ at threshold, we then have

$$\alpha(r) = \frac{0.0063 V_0}{r}$$

and hence

$$A = \exp\left(0.0063 V_0 * \log(\frac{0.06 \frac{V_0}{22}}{15})\right)$$

giving the desired gain in the TRT of $A_{\mathrm{nom}} = 2.5\ 10^4$ for a voltage of 1284 V. This is in agreement with the 1310 V determined from prototype data.

The amplification - a closer look

The above calculation is probably lucky:

- The ionization cross-section is not constant with electron energy. (see Sauli Fig 45).
- Quenching gasses added to the Xe drastically change the cross-section by changing the average kinetic energy of the electrons. (See Sauli Fig 47).

Drift time measurement

- A measurement of the time-lapse between the crossing of the straw by a charged particle and the avalance at the anode wire increases the precision by giving the distance from the crossing charged particle to the wire $r = v_{\mathrm{D}} t$. This is the idea of a drift-chamber (See Sauli Fig 85).
- The TRT records every 3.125ns whether or not the pulseheight measured at the anode is above a certain threshold.

The drift velocity - naive calculation

Assuming the electron is brought to halt at each collision and that the mean free path, λ is independent of energy, we have at a 1mm distance from a TRT wire:

$$\begin{aligned} \lambda &= \frac{1}{2}\frac{eE}{m}\tau^2 \\ \tau &= \sqrt{\frac{2\lambda m}{eE}} \\ v_D &\approx \frac{\tau q E}{2m} \\ &\approx 8cm/\mu s \end{aligned}$$

while the correct answer is about $5cm/\mu s$.

The drift velocity - naive calculation

The difference between prediction and fact is due to:

- Dependence on electron energy of λ, mainly the Ramsauer minimum around 1eV. (See Sauli Fig 24).
- The quencher gas. (See Sauli Figs 25-30)
- The magnetic field (see Sauli Fig 87) bending the drift-trajectories up/down.

Diffusion

- The mean velocity of a particle in an ideal gas is given by Maxwell:

$$v = \sqrt{\frac{8kT}{\pi m}}$$

- According to kinetic theory, a collection of particles localized at $x = 0$ at $t = 0$ later have a distribution:

$$\frac{dN}{N} = \frac{1}{\sqrt{4\pi Dt}} \exp -(\frac{x^2}{4Dt})dx \ ,$$

where D is the diffusion coefficient

Diffusion

- It is also shown (in any text on stat mech), that

$$D = \frac{1}{3} v \lambda \ ,$$

where the mean free path in an ideal gas is:

$$\lambda = \frac{1}{\sqrt{2}} \frac{kT}{\sigma P}$$

- Hence, by substitution

$$D = \frac{2}{3\sqrt{\pi}} \frac{1}{\sigma P} \sqrt{\frac{(kT)^3}{m}}$$

Diffusion of electrons in gases

- In presence of an electric field, electrons and ions will drift with velocity v, proportional to E with a constant of proportionality named the mobility, μ.
- A classical argument by Einstein gives for an ideal gas in thermal equilibrium with the drifting ions:

$$\frac{D}{\mu} = \frac{kT}{e}$$

Diffusion of electrons in gases

- In practice, we parametrize the spread of the coordinate in the drift direction as:

$$\sigma_x = \sqrt{2Dt} = \sqrt{\frac{2\epsilon_k x}{eE}}$$

where the characteristic energy ϵ_k is:

$$\epsilon_k = \frac{eED(E)}{v(E)}$$

- The characteristic energy can be calculated in statistical mechanics using knowledge of the electron-gas collision cross-sections and the average energy loss in each collision (see Sauli equations 15-19).

TRT $r\phi$ resolution

- The gasses in the TRT have a characteristic energy of about 2 eV. Thus we have for the coordinate perpendicular to the wires ($x = r\phi$):

$$\sigma_x = \sqrt{\frac{2 \times 2\text{eV} \times 0.1\text{cm}}{1310/0.2\text{eV/cm}}}$$

  which is $\sigma_x = 124\mu$.

- For an average of 10 primary ion pairs, the radial coordinate of closest one varies by about $\pm 0.15mm$. Thus, the distance of the closest electron to the wire has a spread of $\sigma_x = \frac{1}{2}(0.15)^2$ mm $= 12\mu$.

- The binning of the drift-time in 3.125ns bins contributes $\sigma_x = \frac{1}{\sqrt{12}} \frac{3.125}{42} 2\text{mm} = 43\mu$.

TRT $r\phi$ resolution cont'd

- The noise is about 1400 electrons, compared with the 8000 electrons required to pass the electronic threshold, set at 250 eV energy loss. With a rise-time of 8ns up to about 1.2 keV, this contributes
  $\sigma_x = \frac{1400}{8000}\frac{0.25}{1.2}8\text{ns} \times v_{\text{drift}} = 18\mu$.
- Gain variations due to offsets in the wire position, pressure variations etc are expected to be held below a few % , corresponding to about $\sigma_x = 30\mu$.
- Adding these items together in quadrature gives about $\sigma_x = 135\mu$. In test beam resolutions of about 145μ have been measured.

Multiwire proportial chambers

- In 1968 it was shown by Charpak that an array of many closely spaced anode-wires in the same chamber could each act as a independent proportional counters. This provided a affordable way of measuring particles over large areas, and the technique was quickly adopted in high energy physics. Later it has found applications in all kinds of imaging of X-rays or particles from radioactive decay. See Leo Fig 6.8.

Multiwire proportial chambers cont'd

- The wires are each soldered onto a printed board, containing read-out electronics, which is glued onto a fiber-glass or epoxy frame. To be electrostatically stable, the wire tension must exceed a certain value (see Leo equation 6.42). In the TRT, it is 70g.
- The cathode can be either another wire-array or thin strips of conductor deposited on a mylar sheet. Orienting the strips perpendicular to the wires allows for the simultaneous measurement of the coordinate along the wire by reading out the signal induced on the strips by the slow drift of the positive ions. (See Leo Fig 6.7).

The largest TPC built to date is in the Aleph detector at CERN.

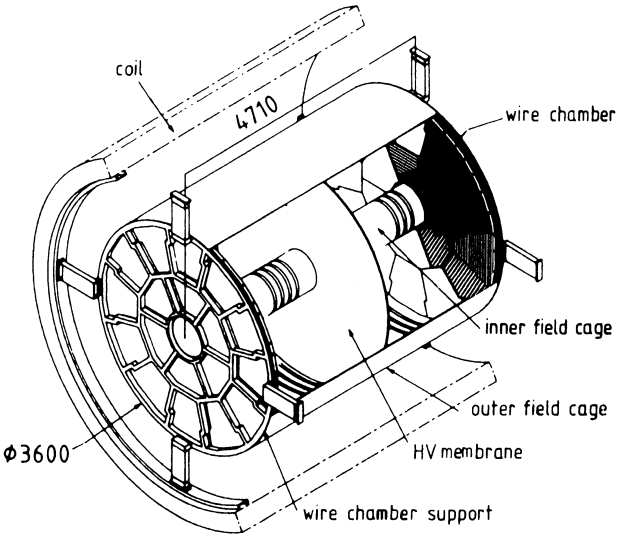

Typical event display

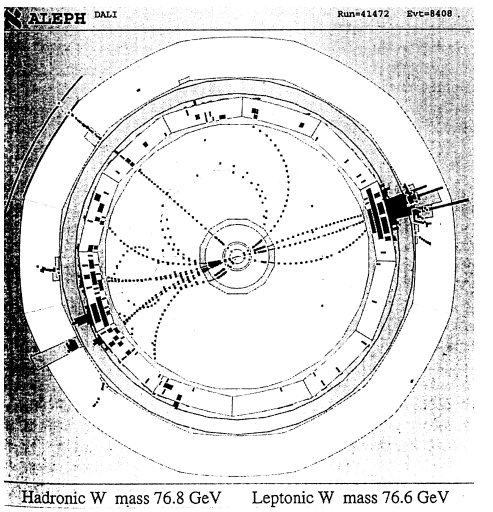

27-1

The TPC Wire Chamber

is a MWPC with typically four planes:

- **The Cathode Plane** are segmented into pads. The mirror charge from the avalance debris, drifting towards the pads, provides the xy coordinate of the hit.
- **The Sense/Field Wire grid** contains alternating sense and field wires. The sense (anode) wires are very thin and at +HV for creating the avalances. The field wires serve to electrically decouple the sense wires.
- **The Potential Grid** serves to prevent positive ions from escape back into the drift volume.
- **The Gating Grid** has two states: Open and Closed. In the Closed state, the wires are placed at alternating potential creating a dipole field to block electrons drifting in and positive ions drifting out. One can Open at a trigger and Close after T_{max}.

Detail of endcap sector

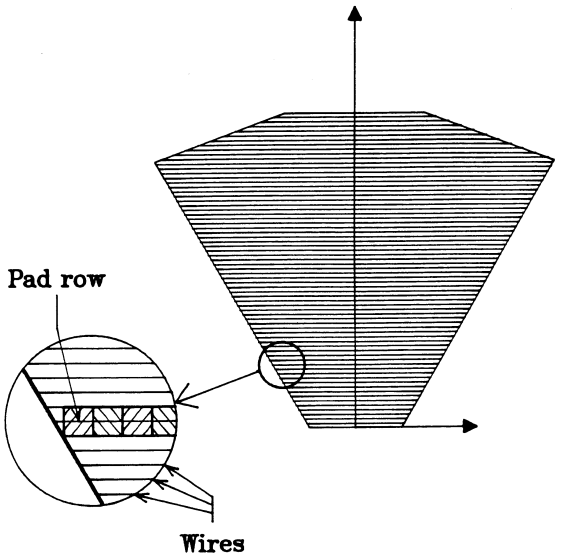

A combination of grids provides
field shaping
avalanching
signal sensing

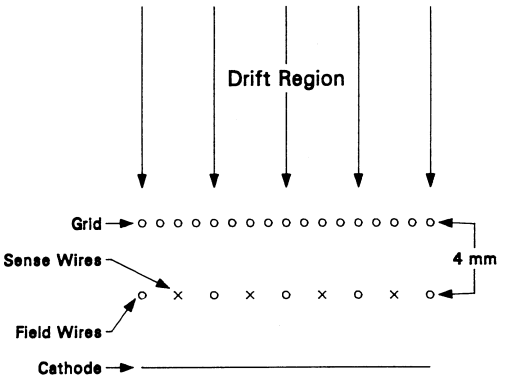

The MWPC in the ALEPH TPC

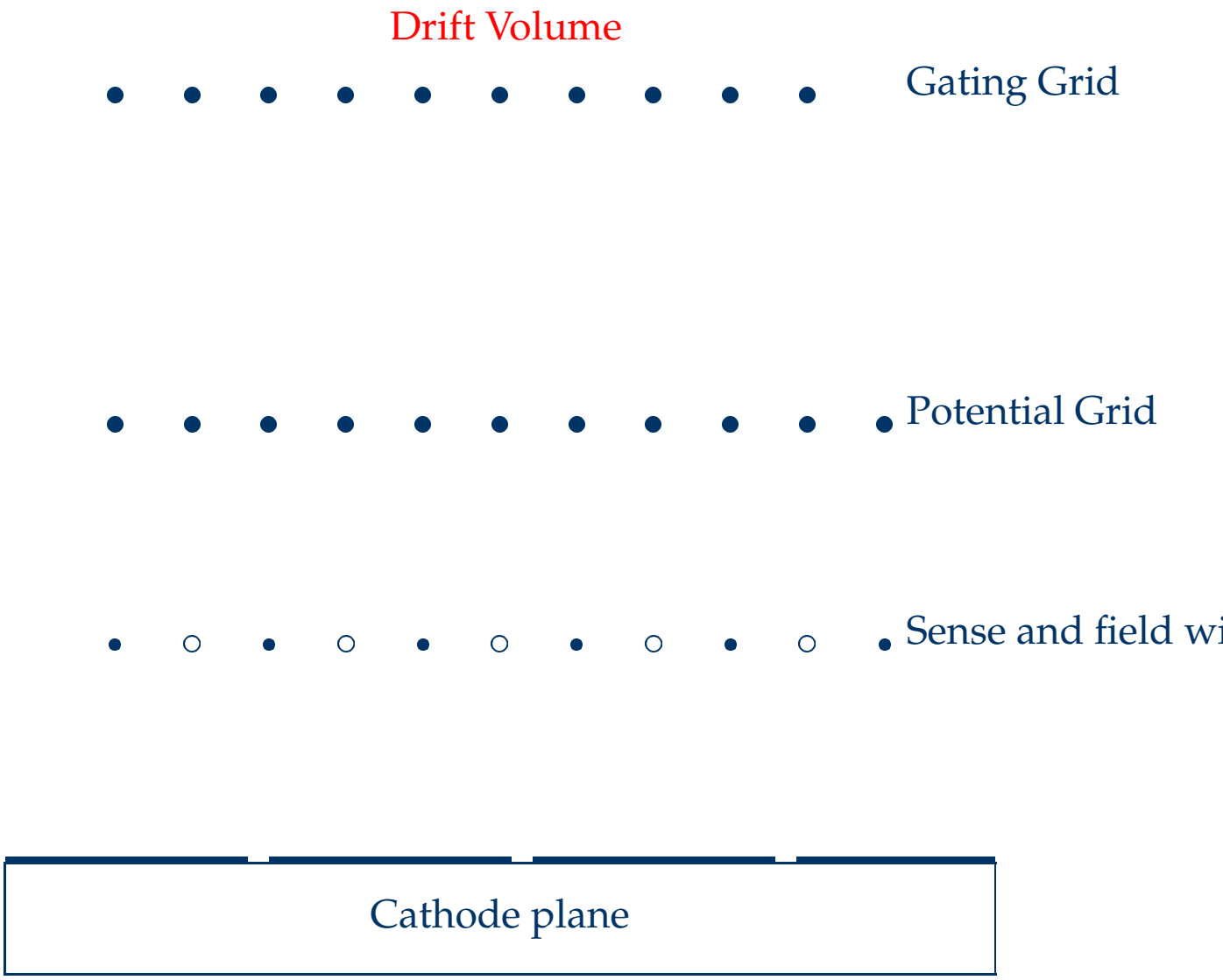

The TPC field cage

Experience shows that the greatest challenge in a TPC is to maintain a constant axial electric field. This field is made by electrodes on the inner and outer cylinders of the Field Cage, connected to a resistor chain. Some useful elements are:

- **A Gating Grid** to avoid space-charges.
- **Tight mechanical tolerances** wrt the ideal cylindrical shape (while keeping the material budget low).
- **Severe cleaniness**, (the tiniest piece of fiber in the cage may short-cut two electrodes and distort the field.)
- **As little as possible of insulator** exposed to the drift-volume to avoid build-up of charge on the insulator.
- **Perfect matching** of equipotential surfaces at the end plane is needed to avoid transverse field components.

Calibration

- **Wire-to-wire gain variations** are calibrated with a source before assembly.
- **The *B*-field** is measured before assembly.
- **Pedestal subtraction** is normally implemented in hardware.
- **Pulsing of field wires** tracks the electronics gains. Non-linearities are ideally corrected in hardware.
- **Laser Calibration** is used for large TPCs to calibrate field-distortions and the drift velocity. Best is a pulsed Nb-YAG, because of its high-power and small wavelength. The small wavelength is needed to reduce the number of photons needed to ionize a gas atom. The high power is needed in order to be able to split the beam into many sub-beams traversing different parts of the TPC.

Electron drift in E and B fields

The TPC is immersed in a magnetic field, $\bar{B}$ parallel to the electric field.
The Langevin equation

$$m\frac{d\bar{v}}{dt} = e\bar{E} + e(\bar{v} \times \bar{B}) + \bar{Q}(t)$$

becomes in the stationary state

$$0 = e\bar{E} + e(\bar{v}_D \times \bar{B}) - \frac{m}{\tau}\bar{v}_D$$

Introducing the mobility, $\mu = \frac{e\tau}{m}$, and the cyclotron frequency, $\bar{\omega} = \frac{e\bar{B}}{m}$, one finds

$$\bar{v}_D = \mu\bar{E} + \tau\bar{v}_D \times \bar{\omega}$$

Electron drift in E and B fields

Solving for $\bar{v}_D$:

$$\bar{v}_D = \frac{\mu E}{1+\omega^2\tau^2}\left[\hat{E} + \omega\tau\hat{E}\times\hat{B} + \omega^2\tau^2(\hat{E}\hat{B})\hat{B}\right]$$

where the "hat" denotes unit vector.

Electron drift in E and B fields

- Since the coordinate resolution is high in the azimuthal direction, a v_D^{ϕ}-component due to field distortions is very dangerous. But high $\omega\tau$ helps!
- At high $\omega\tau$, the electrons drift along the B-field lines !
- At high $\omega\tau$, v_D^{ϕ} is suppressed by powers of $\omega\tau$, except for the effect of a B_{ϕ} component. However, B_{ϕ} is zero on the average according to Ampere.

Diffusion in E and B fields

Recall the longitudinal diffusion, along the field direction (in the thermal limit)

$$D_0 = \frac{1}{3}\frac{\lambda^2}{\tau}$$

In the transverse projection, however, an electron follows the arc of a circle with radius $\rho = v_T/\omega$, where the mean squared velocity projected onto the transverse plane is:

$$v_T^2 = \frac{2}{3}\frac{\lambda^2}{\tau^2}$$

Diffusion in E and B fields

After a time, t, the electron has reached a transverse distance of $2\rho \sin \frac{v_T t}{2\rho}$, and the spread after one collision is:

$$\delta^2 = \frac{1}{2}\int_0^\infty \frac{dt}{\tau} \exp\left(-\frac{t}{\tau}\right)\left[2\rho \sin \frac{v_T t}{2\rho}\right]^2 = \frac{1}{2}\frac{\tau^2 v_T^2}{1+\omega^2\tau^2}$$

Diffusion in E and B fields

After a longer time, the transverse spread is

$$\sigma_T^2(t) = \frac{t}{2}\frac{\tau v_T^2}{1+\omega^2\tau^2} = t\frac{D_0}{1+\omega^2\tau^2}$$

Thus in large magnetic fields

the transverse diffusion is reduced by a factor $1+\omega^2$

e.g. for Ar/CH_4 and $B = 1.5$ Tesla the reduction is a factor 50.
This is what makes a TPC possible!.

Faster and denser gaseous detectors

- At the LHC, bunches collide every 25 ns, giving rise to hundreds or even thousands of particles at each collision. Even at large radii, standard drift-chambers with drift times of the order 1 μs can not be used.
- Silicon pixel and strip detectors can do the job, but they are expensive both in money and rad. lengths – and they are too slow for use in a first level trigger.
- Therefore, new faster types of gaseous detectors with much denser readout have been developed:
  - Straw tubes
  - Thin Gap Chambers
  - MultiStrip Gas Chambers
  - Pixel Gas Chambers
  - Resistive Plate Chambers

From coordinates to tracks

- Consider a tracker with N planes normal to a local z axis. Each plane measures a x and/or a y coordinate. The task is now to determine which coordinates belong to which track and to fit the parameters of each track.
- For a cylindrical detector with an axial magnetic field, the tracks ideally form a helix with parameters $\bar{\alpha}$, e.g.:
  - Signed inverse radius of curvature $\pm 1/R$
  - Closest approach to beam-line d_0, ϕ_0, z_0
  - Polar angle wrt the beam-axis θ

  to be determined from a least-squares fit to the measured coordinates.

From tracks to momenta

- The fitted radius of curvature yields the momentum from the formula:

$$p_T[\mathrm{GeV/c}] = 0.3B[\mathrm{Tesla}]R[\mathrm{m}]$$

  where p_T is the momentum perpendicular to the magnetic field.

- To estimate the momentum resolution, the $1/R$ parameter can be replaced by the sagitta, s:

$$s = R - R\cos\frac{\theta}{2} \approx \frac{R\theta^2}{8}$$

From tracks to momenta

- For small bending angles, we insert $\theta = \frac{L}{R}$, and get

$$s \approx 0.3 \frac{BL^2}{8 p_T}$$

and thus

$$\sigma(\frac{1}{p_T}) \approx \frac{0.3BL^2}{8} \sigma(s)$$

From tracks to momenta

- With three measurements: one in each end and one in the middle, we have $s = x_2 + \frac{1}{2}(x_1 + x_3)$, and thus $\sigma(s) = \sqrt{\frac{3}{2}}\sigma_x$, or

$$\sigma(\frac{1}{p_T}) \approx \frac{33}{BL^2}\sigma_x$$

where σ_x is the uncertainty in each coordinate measurement. In a setup with axial geometry, we measure typically $x = r\phi$.

From tracks to momenta

- With N equidistant measurements, it can be shown that:

$$\sigma(\frac{1}{p_T}) \approx \sqrt{\frac{720}{N+4}} \frac{\sigma_x}{0.3BL^2}$$

- So to make a good momentum measurement, we need
  - A long lever arm (quadratic dependence)
  - A strong field (linear dependence)
  - Precise coordinate measurements (linear dependence)
  - Many coordinate measurements (square-root dependence)

From tracks to momenta

- The momentum uncertainty also gets a contribution from Multiple Scattering. A more handy formula for the rms scattering angle than the one in Leo is the following:

$$\sqrt{<\theta^2_{\mathrm{proj}}>} \approx \frac{21\ \mathrm{MeV}}{2p\beta}\sqrt{\frac{x}{X_0}}\left(1+0.038\log\frac{x}{X_0}\right)$$

  where $\frac{x}{X_0}$ is the amount of material traversed, measured in radiation lengths.

- The corresponding momentum uncertainty is

$$\frac{\sigma(p_T)}{p_T^2} = \frac{\sqrt{<\theta^2_{\mathrm{proj}}>}}{0.3BL}$$

Momentum errors in the ATLAS TRT

- Inserting the relevant numbers from the ATLAS TRT for a high energy particle emitted at 90° to the magnetic field, we get for single isolated tracks a resolution error of

$$\frac{\sigma(p)}{p^2}(res) \approx 6\ 10^{-3}$$

- From multiple scattering, we get

$$\frac{\sigma(p)}{p}(MS) = 0.0014$$

- So multiple scattering dominate the error on the size of the momentum for momenta below 800 MeV for a stand-alone TRT measurement.

Momentum errors in the ATLAS

- When considering the total momentum measurement, including the silicon layers, the multiple scattering will dominate the error up to much higher momenta.
- However, the statistics on e.g. $W^{\pm}$ production at the LHC is expected to so enormous that the Gaussian resolution is of less importance than the possible systematic error on the momenta due to displacements of silicon detector elements and TRT wires. Together with the knowledge of the magnetic field, such uncertainties will probably dominate the error on a measurement of the W mass.